Kinetics of Nucleoside Triphosphate Cleavage and Phosphate Release Steps by Associated Rabbit Skeletal Actomyosin, Measured Using a Novel Fluorescent Probe for Phosphate†

Howard D. White,*,‡ Betty Belknap,‡ and Martin R. Webb§

Department of Biochemistry, Eastern Virginia Medical School, Norfolk, Virginia 23507, and National Institute for Medical Research, Mill Hill, London, NW7 1AA, U.K.

Received March 10, 1997; Revised Manuscript Received July 9, 1997⊗

ABSTRACT: We have measured the kinetics of inorganic phosphate (P_i) release during a single turnover of actomyosin nucleoside triphosphate (NTP) hydrolysis using a double-mixing stopped-flow spectrofluorometer, at very low ionic strength to increase the affinity of myosin−ATP and myosin−ADP−P_i to actin. Myosin subfragment 1 and a series of nucleoside triphosphates were mixed and incubated for ∼1−10 s to allow NTP to bind to myosin and generate a steady state mixture of myosin−NTP and myosin−NDP−P_i. The steady state intermediates were then mixed with actin. The kinetics of P_i release were measured using a fluorescent probe for P_i, based on a phosphate binding protein [Brune et al. (1994) *Biochemistry 33*, 8262−8271]. These data are correlated with quenched-flow data, where the extent of the rapid burst of hydrolysis during the first turnover of ATP hydrolysis was followed by chemical quenching of the reaction mix at various times after rapidly mixing ATP and myosin subfragment 1. From the double-mixing actomyosin measurements, the kinetics of P_i release are biphasic. The fast phase corresponds to P_i release from the associated actomyosin−ADP−P_i complex. The slow phase measures the rate of the cleavage step on associated actomyosin. At saturating actin, there is a correlation between the amplitude of the fast phase and the size of the P_i burst observed by quenched flow in the absence of actin: the size of this phase corresponds to the amount of myosin−ADP−P_i formed during the first mix. For ATP at 20 °C the rate of the P_i release step is 75 (±5) s^{-1}, 25-fold larger than the cleavage step, which is the rate-limiting step of actomyosin ATP hydrolysis at saturating actin. The rate constant of P_i release varies only slightly with nucleoside structure. The rate constant of the slow phase of the P_i release (measuring cleavage) is highly dependent upon the structure of the NTP substrate.

Muscle contraction occurs as the result of cyclic association and dissociation of cross-bridges formed between myosin molecules in the thick filaments and f-actin molecules in the thin filaments, with concomitant hydrolysis of ATP. This cycle can lead to relative sliding of the actin and myosin filaments and the production of work. A rationale for studying the kinetic mechanism of ATP hydrolysis by actomyosin subfragment 1 (S1)[1] in solution is that it may directly relate to the observed physiological and pathological properties of muscle. Scheme 1 contains the generally accepted mechanism of actomyosin ATP hydrolysis in fibers or by the isolated proteins. Because the interaction of actin with myosin in solution is greatly reduced by increasing ionic strength, most studies of the isolated proteins have been at ionic strengths significantly lower than physiological.

Scheme 1

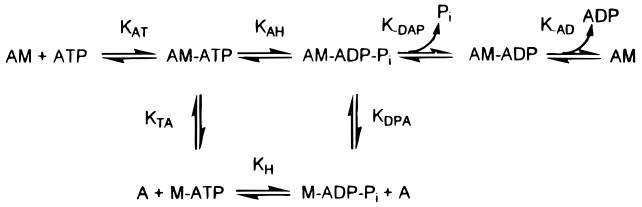

ATP binding to actomyosin is rapid and produces a rapid dissociation of myosin-S1 from actin (>1000 s^{-1}) in dilute solution at physiological ionic strength. The rate of M−ATP hydrolysis to M−ADP−P_i is approximately 100 s^{-1} at 20 °C. The steady state rate of hydrolysis by myosin in the absence of actin is limited by slow release of inorganic phosphate, P_i (*2*). Actin increases the steady state rate of ATP hydrolysis by increasing the rates of product release >100-fold (*3*,*4*). The transitions between weakly bound states, AM−ATP and AM−ADP−P_i, and the strongly bound

† This work was supported by MRC, U.K., the National Institutes of Health (HL41776, AR40964), and the American Heart Association (Virginia Affiliate).

* To whom correspondence should be addressed.

‡ Eastern Virginia Medical School.

§ National Institute for Medical research.

⊗ Abstract published in *Advance ACS Abstracts,* September 1, 1997.

[1] Abbreviations: aza-ATP, 1,N^6-etheno-2-aza-ATP; S1, myosin subfragment 1; A1, the 21 kDa alkali light chain of myosin-S1; AM, actomyosin; NTP, nucleoside triphosphate; mant, 2′(3′)-*O*-(*N*-methylanthraniloyl)-; MOPS, 3-[*N*-morpholino]propanesulfonic acid; DTT, dithiothreitol; PBP, phosphate binding protein; MDCC, *N*-[2-(1-maleimidyl)ethyl]-7-(diethylamino)coumarin-3-carboxamide; PNPase, purine nucleoside phosphorylase; MEG, 7-methylguanosine.

[2] The following nomenclature is used to identify rate and equilibrium constants of the nucleotide hydrolysis mechanism. Positive subscripts identify rate and equilibrium constants of association; negative subscripts identify rate and equilibrium constants of dissociation. Single subscripts (A = actin, T = nucleoside triphosphate, D = nucleoside diphosphate, P = phosphate, and H refers to the hydrolysis of T to D and P) refer to the binding of the respective ligand to myosin-S1, which is abbreviated M. For multiple subscripts, the final letter of the string identifies the ligand associating (or dissociating) and all other letters refer to ligands already bound.

S0006-2960(97)00540-0 CCC: $14.00 © 1997 American Chemical Society

states, AM−ADP and AM, are thought to be associated with movement in fibers and production of force (*5*−*7*).

The mechanism of ATP hydrolysis by actomyosin and its proteolytic fragments has been studied for more than twenty-five years. In spite of intensive investigation by many laboratories, the rate constants of all the elementary steps have not been measured nor has the identity of the rate-limiting step been generally agreed upon. There have been several reasons for these inconclusive results.

(i) Substrate binding weakens the interaction of myosin with actin, so that at physiological ionic strength dilute actomyosin is almost completely dissociated by addition of substrate. Even at the relatively low ionic strength conditions used for most solution kinetic studies there is partial dissociation by substrates. This has made it difficult to determine the rate constants of the hydrolysis and P_i dissociation steps in the presence of actin.

(ii) Until the development of a fluorescent phosphate indicator (*1*) there has not been a chemical or spectroscopic signal associated with the dissociation of P_i from AM−ADP−P_i, with sufficient time resolution to measure this process in real time.

A mutant phosphate binding protein (PBP) from *Escherichia coli* is used here to measure the kinetics of P_i dissociation from actomyosin-S1. Preparation, characterization and initial experiments utilizing the protein have been reported (*1*). A cysteine engineered into the protein at position 197 is covalently labeled with the fluorescent dye, *N*-[2-(1-maleimidyl)ethyl]-7-(diethylamino)coumarin-3-carboxamide (MDCC). The fluorescence emission of the probe (MDCC−PBP) increases ∼8-fold upon saturation by P_i. The protein binds a single P_i with $K_d \sim 0.1$ μM and a second-order rate constant of 1.4×10^8 M^{-1} s^{-1} (20 °C). This large change in emission spectrum as well as the rapid and tight binding makes the protein an ideal probe with which to measure the kinetics of P_i release. Due to the high affinity of MDCC−PBP for P_i and the ubiquitous contamination by this ion, a "P_i mop" utilizing purine nucleoside phosphorylase (*1*) is used in all solutions to reduce contaminating P_i to < 0.1 μM.

EXPERIMENTAL PROCEDURES

Materials. "Bacterial" purine nucleoside phosphorylase (PNPase), 7-methylguanosine (MEG), ATP, CTP, and GTP were from Sigma. MDCC−PBP was prepared as described by Brune et al. (*1*), with modifications (Brune et al., unpublished). MDCC used in the preparation of MDCC−PBP used in this work was prepared by Dr. J. Corrie, but MDCC is now available commercially from Molecular Probes (Eugene, OR). A detailed description of the preparation of MDCC−PBP will be published elsewhere. However, the method can be obtained prior to publication by request from M.W. MantATP and mantCTP were prepared and purified according to published procedures of (*8*). 1N^6-Etheno-2-azaATP was purified according to the procedure of Smith and White (*9*).

Rabbit skeletal actin and myosin were prepared as previously described (*7*). The subfragment 1 was prepared from myosin with chymotrypsin by the method of Weeds and Taylor (*10*) except that 2 mg of lima bean trypsin inhibitor per mg of chymotrypsin rather than PMSF was used to inhibit chymotrypsin. The protein was column purified on DEAE-52 cellulose. Fractions were pooled to obtain myosin-S1 containing only the A1 light chain component.

Kinetic Measurements. Steady state ATP hydrolysis was measured using [γ-^{32}P]ATP (Dupont). Aliquots (0.1 mL) from the reaction were quenched in a solution (0.9 mL) containing 0.5 M NaH_2PO_4, 2 N HCL, and 10% (w/v) powdered charcoal to bind the unhydrolyzed ATP. The charcoal was removed by pelleting with a 2 min spin in an Eppendorf centrifuge. The hydrolyzed [^{32}P]P_i in the supernatant was counted by the Cerenkov method. Steady state hydrolysis of other NTPs was measured colorimetrically (*11*). Reaction velocities were determined from at least four time points per actin concentration by the method of initial rates. The data were then fit to the steady state kinetic equation using a Neader−Melder nonlinear least-squares Simplex routine obtained from Dr. John Rupley at the University of Arizona to which a subroutine had been added for calculating steady state rates for complex kinetic models using a matrix solution of the kinetic equations (*12*). Standard deviations of the parameters were calculated by fitting a quadratic function to the surface about the minimum in parameter space and then using the properties of this function to calculate the variance−covariance matrix for the parameters.

Chemical quench measurements were done using a computer-controlled stepper-motor driven quench-flow apparatus built in this laboratory. Solutions (100 μL) of myosin-S1 and ATP (containing 10 000−20 000 dpm [^{32}P]-ATP) were mixed, held in a delay line for the desired time, and then quenched by a second mix with 2 N HCl to give a final volume of 1.0 mL. A 0.6 mL portion of the sample was mixed with an equal volume of charcoal slurry and centrifuged as described for steady state rate measurements to remove unhydrolyzed ATP. The total radioactivity of ATP in each sample was determined by counting 0.3 mL directly. The percent hydrolysis was obtained from the ratio of the radioactivity in charcoal treated to directly counted samples after subtracting background from each. The data were then fit to a two exponential equation using a Simplex fitting routine to obtain amplitude and rate information. Although the ratio of S1:ATP was only 2:1, a two-exponential fit is an adequate approximation to accurately obtain the amplitude information required to determine the equilibrium constant of the hydrolysis reaction.

Stopped-flow fluorescence measurements of ATP binding to myosin-S1 were made using an Applied Photophysics stopped-flow fluorometer illuminated by a 100 watt mercury lamp. The 295 nm excitation light was selected using a 0.125 m monochromator (Farrand Corporation). Tryptophan fluorescence emission (320−380 nm) was selected using a Corning UG-3 glass filter. Four 1024-point data traces were averaged using a Nicolet Explorer III oscilloscope and transferred to a PC for data storage and analysis. Observed rate constants were obtained by fitting the data to a single-exponential equation using the method of moments (*13*). Stopped-flow experiments measuring P_i release were made using a HiTech SF61MX apparatus in the double-mixing configuration with a mercury lamp, a monochromator with 5 nm slits to isolate 436 nm excitation light, and a 455 nm cutoff filter on the emission. The excitation light had a 1 cm pathlength. Data were fitted to theoretical curves using the HiTech IS-2 software, Enzfitter (Biosoft), Grafit (*14*), or nonlinear least-square fitting using the Simplex method (*15*).

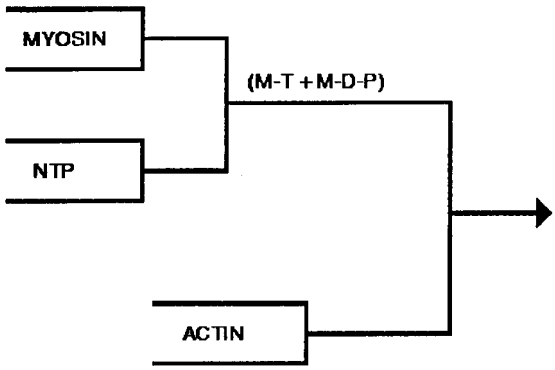

FIGURE 1: Double-mixing stopped-flow experiments. Rabbit skeletal myosin-S1-A1 (16 μM) is mixed with nucleoside triphosphate substrate (8 μM) and allowed to incubate for 1−10 s in a delay line to obtain steady state binding and hydrolysis of substrate. At the end of the delay period the steady state intermediates (M−NTP and M−NDP−P_i) are mixed with actin. Optimum delay times were determined from measured rate constants of substrate binding and steady state rates of hydrolysis.

RESULTS

In this work we have utilized very low ionic strength conditions (1 mM MOPS, 0.4 mM $MgCl_2$) and rabbit myosin-S1 with only the A1 light chain in order to promote the association of M−NTP and M−NDP−P_i with actin. We have used the double-mixing stopped-flow method to generate first a steady state mixture of M−NTP and M−NDP−P_i before mixing with actin as shown in Figure 1. In the first mix, substrate is mixed with 2-fold excess myosin-S1 and incubated for 1−10 s. The optimum incubation time is dependent upon temperature, rates of substrate binding, and steady state hydrolysis in the absence of actin, determined by P_i release. This incubation time was varied in order to maximize the amounts of M−NTP and M−NDP−P_i. Much higher concentrations of myosin-S1 than were required to obtain a good signal/noise ratio were used (16 μM in the syringe, 4 μM in the second mixing chamber) in order to increase the rate of substrate binding to myosin. The incubation time was long enough for >95% of the substrate to bind but not long enough for excessive breakdown of the steady state intermediates to occur. For substrates with relatively rapid rates of binding such as ATP, mantATP, and azaATP, amplitudes were largest after 1 s incubation at 20 °C and decreased with longer times. Substrates with slower rates of binding such as CTP, mantCTP, and GTP required longer times to achieve the maximum extent of binding (5−10 s). Actin binding is rapid and occurs within the dead time of the second mix, and the fate of AM−ATP and AM−ADP−P_i was followed by measuring the kinetics of P_i release. At saturating actin concentrations the observed kinetics of P_i release would be single exponential if P_i release itself is rate limiting for the actomyosin ATPase. If the hydrolysis step is rate limiting, a double exponential may be observed: fast P_i release directly from AM−ADP−P_i followed by slow P_i release for AM−ATP controlled by the cleavage rate.

Kinetics of P_i Release Obtained upon Mixing Steady State Mixtures of M−NTP and M−NDP−P_i with Actin. Data in Figure 2A obtained with ATP as the substrate at 20 °C are fit by two exponentials with rate constants of 3.1 and 74 s^{-1}. These data are evidence that the rate of P_i dissociation from AM−ADP−P_i is approximately 25 times more rapid than the rate of hydrolysis of AM−ATP to AM−ADP−P_i. The measurement was repeated with a range of nucleotide analogues, previously used to investigate the actomyosin ATPase mechanism and fiber mechanics (*15*,*16*). Data obtained with azaATP, mantATP, CTP, mantCTP, and GTP as substrates are shown in Figure 2B−E. A summary of kinetic constants obtained with this series of substrates and various experimental conditions is shown in Table 1. The rate of the fast component varies little, 60−90 s^{-1}, for all six substrates at 20 °C. However, the rate of the slow component and the relative amplitudes of the fast and slow component vary more than 250-fold with substrate. The extremes are >90% slow at 0.02 s^{-1} for GTP and ∼2% slow at 5 s^{-1} for CTP. The amplitude of the fast component and rate of the slow component have the dependence CTP ∼ mantCTP > ATP > mantATP > azaATP > GTP. The rate of P_i dissociation is essentially independent of substrate, whereas the rate and equilibrium constants of the cleavage step in the presence and absence of actin are very sensitive to substrate structure. A comparison between the rate constant of the cleavage step, k_a, and the steady state rate of hydrolysis at saturating actin, k_{cat} in Table 1, indicates that the cleavage step is the rate-limiting step at saturating actin.

During the first mix, in the absence of actin, P_i release is slow and the amounts of M−NTP and M−NDP−P_i represent the relatively rapid (steady state) equilibrium between these species. After the second mix, actin binds rapidly to each intermediate, so that the relative amplitudes of the slow and fast components of the observed P_i released should be a measure of the equilibrium constant between M−NTP and M−NDP−P_i in the absence of actin. A comparison of the amplitudes of the equilibrium constant of the hydrolysis in the absence of actin with the ratio of slow to fast components shown in Table 1 is consistent with such a mechanism. The observed ratio of the amplitudes of the fast to slow phases of P_i dissociation increases with temperature as expected because the hydrolysis equilbrium constant, K_H, for ATP is more favorable to products at higher temperature (*17*). There is little if any "phosphate burst" for GTP hydrolysis by myosin-S1, measured by quenched flow (*18*). The amplitude of P_i release observed here is <10% of the total signal, indicating that M−GTP is the predominant steady state intermediate. The equilibrium constant for CTP hydrolysis while bound to myosin-S1 is the most favorable for products of any nucleotide so far measured (*19*). Figure 2C shows that there is very little slow phase of P_i release in the double-mixing experiments with CTP indicating that M−CDP−P_i is the predominant steady state intermediate.

To make a more precise quantitative test of the mechanism we have made single-turnover kinetic measurements of ATP hydrolysis using rapid chemical quench methods to directly determine K_H under the same ionic conditions as the P_i release experiments (Figure 3A). The rapid initial hydrolysis of ATP is due to rapid binding and hydrolysis of ATP by myosin to produce M−ADP−P_i. The slower phase is from slow product dissociation, which limits the decay of the steady state intermediates. The equilibrium between M−ATP and M−ADP−P_i at 10 °C in the absence of actin is determined from the ratio of fast/slow amplitudes to be 1.5, which is in reasonable agreement with the equilibrium constant of 1.3 estimated from the amplitude ratio in P_i release experiments in Table 1. The rate constant of the hydrolysis by myosin-S1 can be determined from the observed rate of the increase in tryptophan fluorescence enhancement associated with ATP binding to and hydrolysis

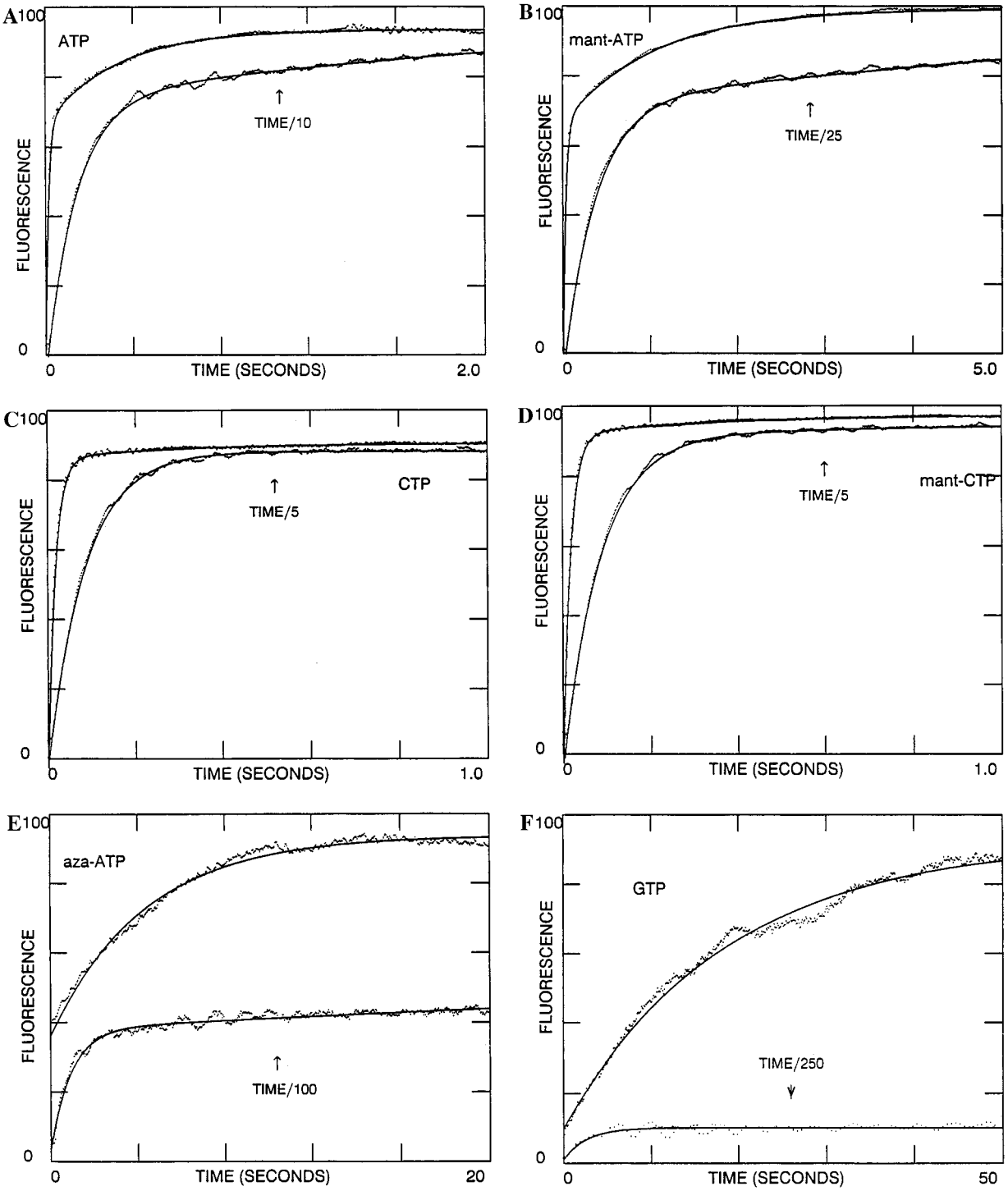

FIGURE 2: Biphasic kinetics of phosphate release. Double-mixing experiments were done as described in Figure 1. Data were obtained over sufficient time for the reaction to go to completion (upper curves). The lower curves have a full scale of 200 ms. The solid lines through the data are best fits to the equation $I(t) = I_a e^{-k_a t} + I_b e^{-k_b t}$. Experimental conditions (second mixing chamber concentrations): 1 mM MOPS, 0.4 mM $MgCl_2$, pH 7.0, 4 μM myosin-S1, 2 μM NTP (as indicated), 50 μM actin at 20 °C. All solutions contained 9 μM MDCC−PBP, 100 μM 7-methylguanosine, and 0.02 unit of PNPase mL^{-1} except for experiments with GTP which contained 0.002 unit mL^{-1}.

by mysoin-S1 (*16*) shown in Figure 3B. The rate observed at saturating ATP concentration ($k_{+H} + k_{-H}$) is ~20 s^{-1} at 10 °C (Figure 3C). Combining the rate and equilibrium data enables the forward and reverse rate constants of the hydrolysis in the absence of actin to be determined as 12 and 8 s^{-1}. Rate constants for the hydrolysis of CTP under similar conditions are 23 and 7 s^{-1}.

Dependence of the Rate of P_i Release upon Actin Concentration. The data in Figure 4 show the dependence of the observed rates of P_i release upon actin concentration. The observed rate of the fast component increases at low actin and reaches a maximum above 20 μM actin. The rate of the slow component reaches a maximum at moderate [actin] and then decreases to a rate that is independent of actin concentration. This kinetic behavior is qualitatively explained by the more rapid hydrolysis step by myosin than actomyosin. At subsaturating actin concentrations, the M−ATP and M−ADP−P_i are partially dissociated from actin and P_i release from M−ATP is controlled by the flux through the fast dissociated cleavage steps followed by actin accelerated P_i release. At saturating [actin] P_i release from M−ATP is controlled by the slower associated cleavage step.

Table 1: Comparison of the Rate Constants of P_i Dissociation and Steady State Hydrolysis for a Series of NTP Substrates[a]

$$AM{-}ATP \xrightarrow{k_a} AM{-}ADP{-}P_i \xrightarrow{k_b} AM{-}ADP + P_i$$

NTP	temperature (°C)	I_b[b] (%)	k_b (s^{-1})	k_a (s^{-1})	k_{cat}[c] (s^{-1})
ATP	4	50	23 ± 1	0.44 ± 0.04	0.35 ± 0.05
ATP	10	56	36 ± 2	0.90 ± 0.05	0.74 ± 0.08
ATP	20	72	77 ± 6	3.1 ± 0.1	2.5 ± 0.4
ATP	30	82	137 ± 5	5.6 ± 0.5	6.7 ± 0.5
CTP	20	97	60 ± 1	5.5 ± 1	5.0 ± 1
mantCTP	20	95	57 ± 1	2.7 ± 0.5	3.1 ± 0.5
mantATP	20	71	61 ± 3	1.9 ± 0.1	2.0 ± 0.3
azaATP	20	33	45 ± 5	0.2 ± 0.02	0.12 ± 0.02
GTP	20	5	60 ± 20	0.02 ± 0.002	0.03 ± 0.001

[a] Experimental conditions are described in Figure 2. [b] Percentage intensity of k_b. [c] Measured at saturating actin.

The rate constants show very little change upon increasing the actin concentration above 20 μM, indicating that the measured processes are first order.

Steady State ATP Hydrolysis. Figure 5 shows the steady state hydrolysis of ATP by actomyosin-S1 measured under the same experimental conditions as were used in the presteady state experiments of Figures 2A and 3. The solid curve through the data was obtained by fitting a solution of the steady state rate to eq 1 as described in the Discussion. The data can be further tested for consistency with the kinetic mechanism by making a comparison of the dependence of k_{obs} upon [actin] in Figure 5 with the dependence of the slow phase of the phosphate transient, k_a, upon actin in Figure 4. They should show the same actin dependence as $k_{obs} = k_a k_b/(k_a + k_b) \sim k_a$. Overall the agreement is remarkably good considering the experiments were done with different protein preparations in different laboratories by different methods. The k_{obs} of both the steady state (Figure 5) and the slow component of the phosphate release (Figure 4) increase with actin concentration and reach a maximum. At higher actin concentrations k_{obs} decreases to a value that is independent of actin concentration. The maximum k_{obs} and k_{obs} at saturating actin agree within 20% with k_a, which is within experimental error. The data are in less good agreement at lower actin concentrations where the k_{obs} obtained by the steady state experiments are initially higher and reach a maximum at lower actin concentrations. This is likely to be due at least in part to differences in free actin concentrations in the two different experiments at low total actin concentrations and increased error in fitting the data for the P_i release experiments at low [actin] where the rate constants of the slow and fast components are less clearly resolved.

DISCUSSION

The results presented here show that at saturating actin the hydrolysis step is rate limiting for associated actomyosin ATP hydrolysis. P_i release is 25−50 times faster. The forward rate of the hydrolysis step is slower when actin is bound to myosin than in the absence of actin. There are sufficient data to determine the rate constants of elementary steps of the ATP hydrolysis mechanism, shown at 10 °C in Scheme 2. Rate constants for the hydrolysis step in the presence of actin ($k_{AH} = 0.7\ s^{-1}$) and the dissociation of P_i from AM−ADP−P_i ($k_{-DAP} = 35\ s^{-1}$) are from Table 2. Rate constants for the hydrolytic step in the absence of actin ($k_H = 12\ s^{-1}$ and $k_{-H} = 8\ s^{-1}$) were measured in Figure 3. Rate constants for ATP binding and ADP dissociation were assumed to be rapid relative to the hydrolysis and P_i dissociation. The solid line drawn through the data was obtained by fitting the data to steady state solutions for Scheme 1 in which the equilibrium constants (K_{TA} and K_{DPA}) for M−ATP and M−ADP−P_i binding to actin were varied to obtain the best fit to the experimental data. The fit values of $10^6\ M^{-1}$ for M−ATP binding to actin and $5 \times 10^4\ M^{-1}$ for M−ADP−P_i binding indicate a 20-fold higher affinity for M−ATP than M−ADP−P_i. The fitting of these two parameters is quite robust as fixing either parameter at a value of half or double the best fit value and fitting the data with only one parameter gave fits that were significantly poorer. The reverse rate constant of the associated hydrolytic step, k_{-AH}, is estimated from detailed balance to be $\sim 7\ s^{-1}$, very similar to that for dissociated hydrolysis. This results in the equilibrium favoring M−ADP−P_i less when actin is bound.

The assignment of the rate constants of P_i dissociation and hydrolytic steps to the observed fast and slow components of the observed rates of the fluorescence enhancement is true strictly only if k_{AH} and k_{-DAP} are the only kinetically significant steps affecting P_i release from AM−ATP and AM−ADP−P_i generated in the double-mixing experiments described in Figure 1. That is if k_{-DAP} (the rate constant of the P_i dissociation step) $\gg k_{-AH}$ (the rate constant of the reverse of the associated hydrolysis step) and k_{AH} (the rate constant of the associated hydrolysis step) $\gg k_{-AT}$ (the rate constant of ATP dissociation from AM) then $k_{AH} \sim k_a$. Here we have found that the P_i dissociation step is $\sim$5-fold faster than the reverse of the hydrolysis. We have used simulations of the rate of P_i dissociation to determine the effect of partial reversibility of the hydrolysis step on the measured rate constants and amplitudes. Increasing k_{-AH} from 0 to $7\ s^{-1}$ increases the predicted rate of the fast component by approximately 20% and decreases the predicted rate constant of the slow component by approximately 10%. Inclusion of a reverse step of $7\ s^{-1}$ also decreases the predicted ratio of fast to slow amplitudes obtained in the P_i release experiments from 1.5 (assuming no reversal) to 1.0. The experimental data gave ratios of fast to slow components from double-mixing experiments of 1.3, which supports the assumption that $k_{-DAP} \gg k_{-AH}$.

Sleep and Hutton (*20*) found that the second-order rate constant of M−ATP binding to actin was approximately one-third that of M−ADP−P_i binding to actin in double-mixing experiments in which the ratio of substrate to product in solution was determined after M−ATP and M−ADP−P_i were mixed with actin. The rate constants of ATP dissociation from AM estimated from their data, $0.5-1\ s^{-1}$ at 10 °C and $2-3\ s^{-1}$ at 20 °C, are comparable to measured values for k_a for ATP in Table 1. If $k_{-AT} > k_{AH}$, AM−T is partitioned between AM−D−P and AM+T. Thus substrate dissociation could be kinetically significant and alter the interpretation of k_a as a measure of the associated hydrolysis reaction. Modeling the reaction shows that if $k_{-AT} > k_{AH}$ and k_{AT}[AM], the rate of rebinding of substrate to AM can limit the slow phase of phosphate release. However, if the rebinding of the dissociated ATP to AM is faster than the rate of dissociation, the effect of this step upon the slow phase of the phosphate release is insignificant. The observed rate of ATP binding to AM ($k_{app} = k_{AT}$[AM]) during the reaction can be calculated from the second-order rate constant k_{AT}, $4 \times 10^6\ M^{-1}\ s^{-1}$, and the estimated concentration of AM present during the slow phase of the hydrolysis reaction

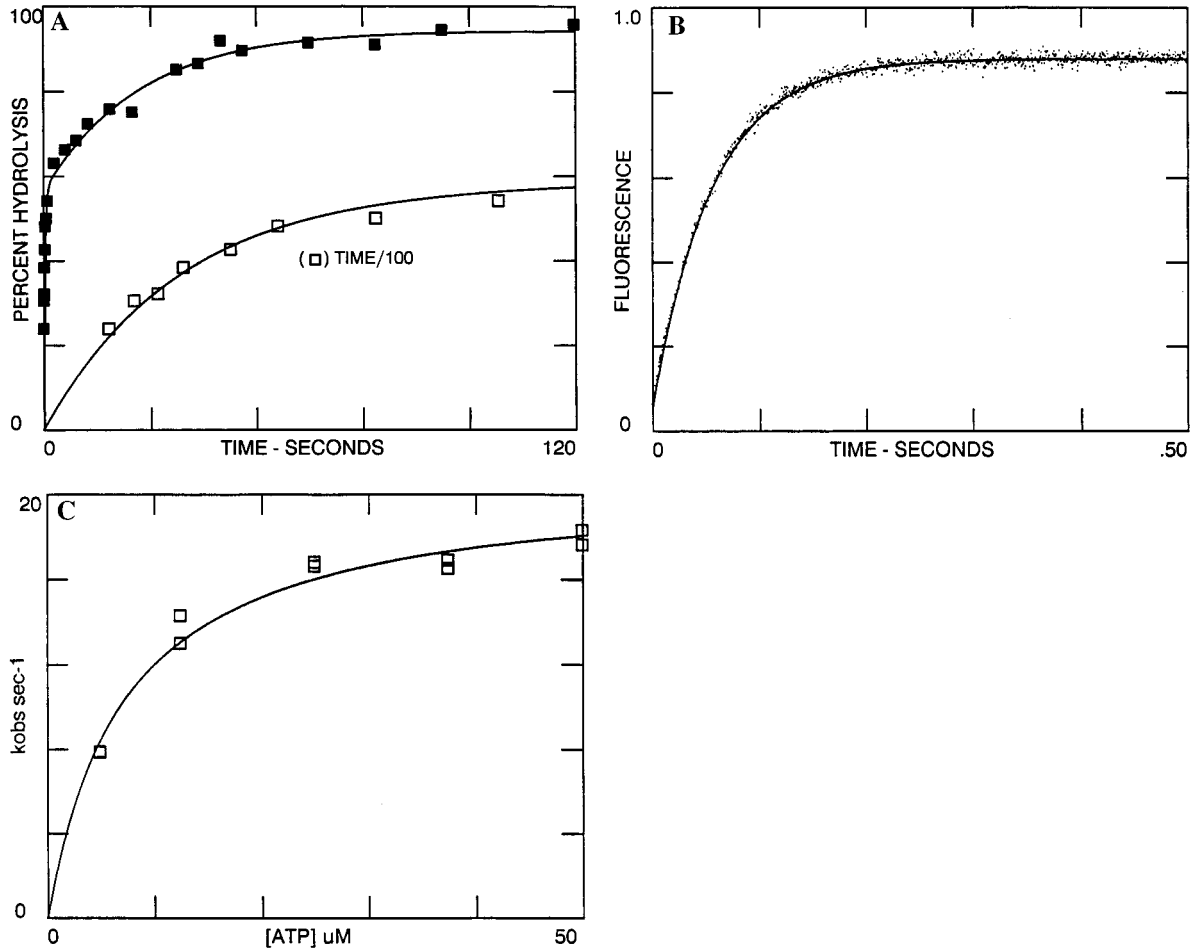

FIGURE 3: Presteady state kinetics of the hydrolysis of ATP by myosin-S1. (A) Measurement of the hydrolysis of a single turnover of ATP by myosin-S1. Experimental conditions: 2 μM myosin-S1, 1 μM ATP, 1 mM MOPS, 0.4 mM $MgCl_2$, pH 7.0, 10 °C. The solid curve through the experimental data are for the equation $I(t) = 59e^{2.6t} + 39e^{0.042t}$. (B) Tryptophan fluorescence enhancement observed upon ATP binding to myosin-S1. Experimental conditions were identical to those in A except that the ATP concentration was 50 μM. The solid curve drawn through the data is a single-exponential fit with $k_{obs} = 18.3$ s^{-1}. (C) The dependence of the observed rate constant upon ATP concentration. Experimental conditions are identical to those in B except that the ATP concentration was varied as indicated. The solid line through the data is a fit of the data to the equation $k_{obs} = k_a/(1 + (K_o/[ATP]))$, where $k_a = 19.6$ s^{-1} and $K_o = 6.2$ μM.

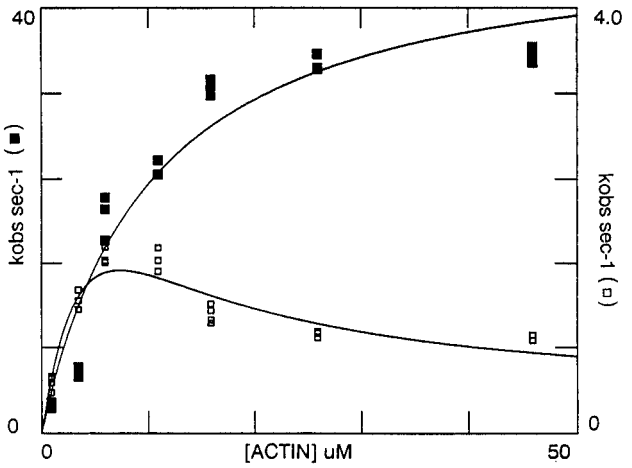

FIGURE 4: Dependence of the slow and fast components of P_i release upon actin concentration. The data were obtained in experiments similar to those shown in Figure 2 except that the temperature was 10 °C, the NTP was ATP, and the total [actin] in the stopped-flow cell was varied as indicated. Solid symbols are for the slow component, and open symbols are for the fast component.

is ~12 s^{-1} at the experimental conditions of Figure 3. This is significantly greater than the expected rate of ATP dissociation from AM−ATP. We have checked the assumption that $k_{AMT}[AM] > k_{-AMT}$ by varying the initial concentration of myosin-S1 mixed with ATP from 4 to 16 μM. The kinetics of phosphate release (observed rate constants and fraction amplitudes) are independent of [myosin-S1] over this range (data not shown). This provides strong experimental evidence that the slow phase of phosphate release, k_a, is measuring the rate of the attached hydrolysis rate, k_{AH}, for ATP and that the rate of ATP dissociation from AM is < 3 s^{-1} at 10 °C. This is consistent with the value of 0.5−1 s^{-1} estimated from Sleep and Hutton's data (*20*). Similar calculations for GTP give k_{app} for rebinding rates of 0.6 s^{-1}, which is ~30-fold faster than k_a, the observed rate of the slow phase of phosphate release, 0.02 s^{-1}. For CTP the value of 5 s^{-1} measured for k_a is sixteen times faster than the rate of CTP binding, 0.3 s^{-1}. The rate of substrate binding is 10-fold different from the slow phase of the phosphate signal for all of the substrates in Table 1, and there cannot therefore be a significant fraction of substrate that dissociates from AM−T and rebinds for any of these substrates. This indicates that the k_a measured for CTP and GTP is an accurate measure of the associated hydrolysis rate, k_{AH}.

The maximum observed rate for the dissociation of AM by ATP is on the order of 1000−2000 s^{-1} (**7**) which indicates that the second-order rate constant of M−ATP binding to actin is (1−2) × 10^9 M^{-1} s^{-1}, near the diffusion limit of reactions between large protein molecules. The rates of release of both products P_i and ADP are increased ap-

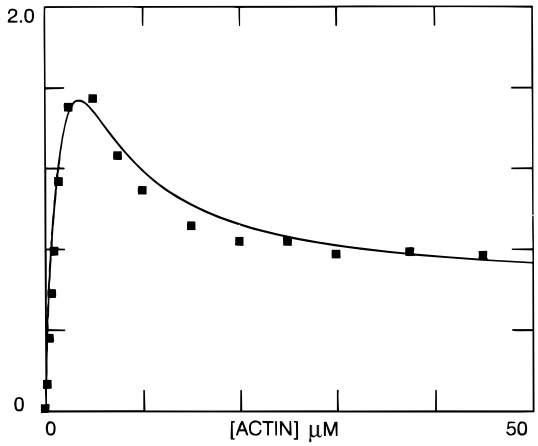

FIGURE 5: Dependence of steady state hydrolysis rate on actin concentration. The k_{cat} for steady state hydrolysis was determined at 10 °C from the hydrolysis of [^{32}P]ATP at ionic conditions similar to those used in the double-mixing experiments in Figure 4 and Table 1 except that the ATP concentration was 200 μM. The line drawn through the steady state data was calculated by fitting the data to the rate constants for the mechanism in Scheme 2 using a Simplex minimization of a matrix solution for the mechanism. The rate constants shown in the Scheme 2 were held constant, and the steady state rate data fit by allowing the equilibrium constants for M−ATP and M−ADP−P_i (K_{TA} and K_{DPA} in Scheme 1) binding to actin to vary. The fit to these two equilibrium constants is very robust with the best values of 1.1×10^6 M^{-1} for M−ATP binding to actin and 5.0×10^4 M^{-1} for M−ADP−P_i. The rate constant for AM−ADP−P_i to AM−ATP (k_{-AH}) was obtained from microscopic reversibility.

Scheme 2

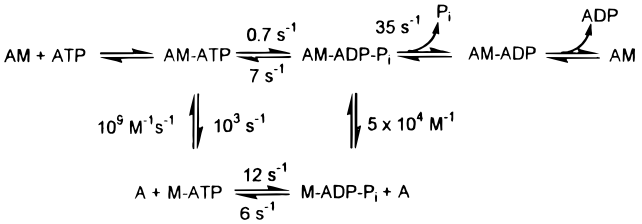

proximately 1000-fold by actin. It is apparent from this mechanism that the maximum rate of steady state hydrolysis, corresponding to the highest point on the curve in Figure 4, does not correspond simply to any rate constant in the mechanism but is rather a compromise between the increase by actin of the rates of product dissociation and the inhibition by actin of the ATP cleavage rate.

These results are in essential agreement with the original Lymn−Taylor mechanism in which the chemical hydrolysis step was thought to occur much more rapidly on myosin than actomyosin (*3*). Rosenfeld and Taylor (*21*) estimated the rate constants of P_i dissociation from AM−ADP−P_i, k_{-DAP}, to be to be 85 s^{-1} and AM−ATP to AM−ADP−P_i, k_{AH}, to be 12 s^{-1} at 20 °C from presteady state ATP hydrolysis and steady state kinetic data. These values can be compared to directly measured values of 77 and 3.1 s^{-1} in Table 1 at the same temperature and slightly lower ionic strength. The agreement with the value for the P_i dissociation step is remarkably good. The 4-fold difference in the rate constant for the hydrolysis step, k_{AH}, might be due to differences in the ionic strength, but we found less than a 20% change in the rate of the hydrolysis by dissociated myosin on changing ionic strength in this range (data not shown) and believe that the difference is more likely to be due to uncertainties in obtaining the rate constant by their indirect fitting methods.

An Arrhenius plot of the temperature dependence of the rates in Table 1 gives energies of activation of 48 kJ mol^{-1} (SEM 1.4 kJ mol^{-1}) for P_i release and 70 kJ mol^{-1} (SEM 6.7 kJ mol^{-1}) for the cleavage step. This compares with 103 kJ mol^{-1} for steady state actomyosin-S1 ATPase activity (*22*) and 100 kJ mol^{-1} for the measurement of P_i release by actomyosin-S1 at slightly higher ionic strength (∼12 mM), where the observed rate (10 s^{-1} at 22 °C) in a single-mix measurement was probably limited by a combination of cleavage and P_i release steps (*1*). In the latter measurements, the modeled rate constant for P_i release is consistent with the value obtained directly here. At the higher ionic strength, presumably most cleavage occurs when actomyosin is dissociated, giving the higher steady state rate.

The rate of P_i release varies only little (<2-fold) with substrate whereas the rate constant of the hydrolysis step catalyzed by actomyosin is highly dependent (>100-fold variation) upon substrate structure and is much slower for poor substrates such as azaATP and GTP. A similar dependence of the equilibrium constant of the hydrolytic step of dissociated myosin-S1 is obtained from the ratio of the amplitude of the slow and fast components of P_i release, which indicate an equilibrium constant of approximately 0.1 for GTP and 40−50 for CTP (Table 1). It is perhaps not surprising that the single step which is most strongly affected by the structure of the substrate is the chemical step, which is likely to require precise alignment of substrate and catalytic groups in the active site of the enzyme for maximal activity. Changes in the structures of the base have a much larger effect than ribose modification of the substrates. The relative stabilization of products to substrate for CTP or ATP relative to GTP of 2.5−3.5 kcal mol^{-1} is almost exclusively due to an increase in the rate of k_H, k_{-H} being essentially independent of NTP structure. The most obvious difference between substrates such as CTP and ATP compared to GTP is the 6′-amino group present in adenine (4′ in CTP) which is replaced by a carbonyl in GTP. These results suggest that this group might have a stabilizing interaction in the active site after cleavage of NTP to NDP−P_i and may be partially explained by the hydrogen bond between the 6′-amino group of ADP and Tyr 135 in the active site of myosin ADP−AlF_4, ADP−beryllium fluoride, and ADP−vanadate complexes (*23*). Tyr 135 is present in the active site of all myosin II sequences and in >90% of all myosins (*24*). Tyr 135 is also positioned to function as a hydrogen bond donor to Tyr 116, which is also highly conserved and present in all myosinII sequences. Figure 6 shows the hydrogen bonds formed between ADP and Tyr 135 (3 Å) and between Tyr 135 and Tyr 116 (2.8 Å) in the active site of dictyostelium catalytic subfragment (*23*). Part of the connecting sequence between the two tyrosine residues forms a segment of antiparallel sheet (residues 117−125). Side chains from the remainder of the sequence form much of the nucleotide binding cleft (residues 126−134). Relative small movements of the base are required for CDP to make similar hydrogen bonds. The bases of etheno-aza-ADP and GDP do not have a 6′-amino group available to be H bond donors to Tyr 135.

These data also show that actin association decreases the forward rate constant of the hydrolytic step ∼20-fold. The structural basis for this decrease is unknown. Furthermore, the physiological significance for such a mechanism with alternative pathways for hydrolysis and its relevance to muscle contraction is not clear. Does the binding of actin slow down the hydrolysis step so that in muscle fibers the

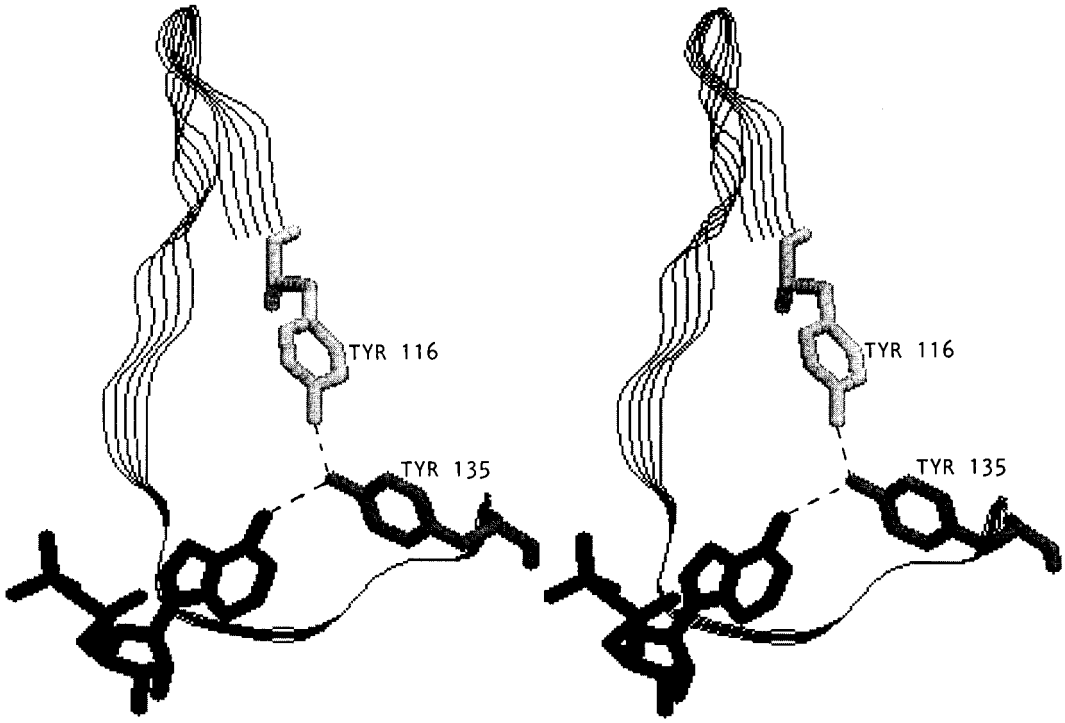

FIGURE 6: An expanded stereoscopic view of the nucleotide binding site of myosin-S1 showing probable H bonding (dotted lines) between the N6 of the base of ADP with Oη of Tyr 135 and between OH of Tyr 135 and Oη of Tyr 116. Coordinates for the structure are of the ADP−BeF_4 complex with dictyostelium catalytic subfragment obtained from the Brookhaven Protein Data Bank (Fischer, 1995) and displayed using Rasmol, version 2.6.

associated pathway is kinetically insignificant under all conditions? Alternatively, does the difference in hydrolysis kinetics represent a mechanism whereby in muscle partition between pathways varies with conditions? While cyclical actomyosin dissociation is presumably essential during shortening, the associated pathway may allow some cross-bridges to remain attached, but hydrolyze ATP slowly, in the isometric state.

The rate of P_i release observed in solution is very similar to the rate of P_i dissociation observed during oscillatory work by fibers hydrolyzing ATP or CTP (M. Kawai and H. White, unpublished data), using MDCC−PBP in contracting fibers (*25*) and by fiber mechanics measurements utilizing caged phosphate (*26*,*27*). Previous work (*28*) showed that the rate of steady state hydrolysis in isometric fibers for a series of substrates is very similar to the maximum steady state rate in solution at very low ionic strength. These data suggest that the associated cleavage step contributes to rate limitation in isometric fibers as well as in solution at saturating actin. Recent data obtained using the phosphate binding protein, in isometric, glycerinated rabbit psoas fibers following photolytic release of ATP, showed that the initial rate of hydrolysis of ATP is fast and within a factor of 2 of the values obtained here for P_i release in the range 5−20 °C (*25*). Although the ionic strength is very different in the two sets of data, they suggest that P_i release may be partially rate limiting for the first few turnovers in isometric fibers and that the slow hydrolysis step on associated actomyosin is circumvented by the more rapid hydrolysis on dissociated cross-bridges. The steady state rate in isometric fibers is 2 −3 s^{-1} (*29*−*31*), a large decrease from the rate for the first few turnovers. The question of magnitude of the bound P_i burst in fibers was addressed by Ferenczi et al. (*32*) and Ferenczi (*33*). The original data showed a large burst at 12 °C, and the data were reconsidered in He et al. (*25*), who determined that the burst may be considerably smaller than the myosin concentration. Myofibrils, either Ca^{2+}-activated or cross-linked, have a bound P_i burst and the cleavage step is approximately one order of magnitude faster than P_i release (*34*−*36*). There is little, if any, bound P_i burst associated with ATP hydrolysis by rabbit skeletal actomyosin in solution at low ionic strength or by cross-linked actomyosin-S1 (*21*, *22*, *37*). The mechanism, which we have determined here in solution, would have little bound P_i burst because the associated hydrolysis step is rate limiting at saturating actin. It is clear that the apparently conflicting results obtained between fibers, myofibrils, and solution studies need resolution, but the partitioning between different pathways and the size of such features as the P_i burst can be significantly altered by rather small changes in rate constants. Such changes are inherent in comparing different protein preparations, particularly as changes in experimental conditions may occur by the nature of the preparation.

A rationale for studying the reaction of different NTP substrates is to determine how the changes in kinetic mechanism affect fiber mechanics and hence provide insight into the relationship between these processes. The unloaded shortening velocity is substrate dependent when measured either in skinned fibers or with the in vitro motility assay (*16*,*38*,*39*). The rate constant of conformational change and the subsequent dissociation of the corresponding NDPs from AM−NDP (*40*) or the rate of P_i release (this paper) do not vary significantly with a range of NTPs, and there is no correlation with shortening velocity. Product release steps are therefore unlikely to be responsible for the differences in shortening velocity observed with different substrates. The rate and equilibrium constants of the hydrolytic steps (K_H and K_{AH}, Scheme 1) vary more than 100-fold with substrate and these changes most likely affect the proportion and flux of biochemical intermediates present and hence fiber mechanics. Changes in the rate of rapid force recovery following rapid stretch and relaxation with different sub-

strates are consistent with recovery being limited by the NTP cleavage step (*41*). It is also relatively straightforward to see how limiting the rate and or equilibrium constants of the hydrolytic steps would be likely to reduce isometric force levels in muscle by reducing the number of cross-bridges in strongly bound force-producing intermediates (AM−D′ to AM) in Scheme 1. Such an affect has been observed using the same series of NTPs in skinned fibers (*16*). If the rate of cross-bridge attachment, which is probably limited by the conversion of M−NTP to M−NDP−P_i, were reduced and the rate of detachment remained unchanged, the primary result would be a reduction in the proportion of attached cross-bridges with little if any effect upon maximum shortening velocity. Both shortening velocity and force are observed to change by about the same amount upon changing NTP (*16*). This type of behavior has been interpreted to imply the presence of an internal load (either within the structure of the fiber or from weakly attached cross-bridges) that prevents low numbers of force-producing cross-bridges from obtaining maximum shortening velocity (*42*). The number of weakly attached AM−NTP cross-bridges would be increased by a reduction in the rate and/or equilibrium constant of NTP cleavage. This would increase the internal load and hence reduce the maximum shortening velocity.

In conclusion, the data presented here along with a body of previous data have allowed a fuller kinetic description of the actomyosin ATPase mechanism (Scheme 2) in solution than has hitherto been possible. Of necessity, this is for a set of conditions (very low ionic strength) in which rate constants are experimentally accessible, and hence extrapolation is needed to other conditions particularly to those relevant to muscle fibers. In addition, the effect of mechanical properties on rate constants is not clear, and this further complicates detailed comparison with kinetic data from muscle fibers. This adds to the importance of having a series of data using different nucleotide substrates. With these provisos, we have attempted to correlate these kinetic data from solution with measurements in fibers, to suggest evidence of whether hydrolysis or release of P_i or ADP is associated with various processes within the fiber. While some data are consistent with a physiological role for hydrolysis by associated actomyosin, further work is needed to establish this possibility, particularly to understand the variation in ATPase activity in muscle with mechanical conditions and during onset of the isometric state.

REFERENCES

1. Brune, M., Hunter, J. L., Corrie, J. E. T., and Webb, M. R. (1994) *Biochemistry 33*, 8262−8271.
2. Bagshaw, C. R., and Trentham, D. R. (1973) *Biochem. J. 133*, 323−328.
3. Lymn, R. W., and Taylor, E. W. (1971) *Biochemistry 10*, 4617−4624.
4. Siemankowski, R. F., and White, H. D. (1984) *J. Biol. Chem. 259*, 5045−5053.
5. Geeves, M. A. (1992) *Philos. Trans. R. Soc. London, Ser. B 336*, 63−70.
6. Stein, L. A., Schwarz, R. P., Jr., Chock, P. B., and Eisenberg, E. (1979) *Biochemistry 18*, 3895−3909.
7. White, H. D., and Taylor, E. W. (1976) *Biochemistry 15*, 5818−5826.
8. Hiratsuka, T.(1983) *Biochim. Biophys. Acta* 742, 496−508.
9. Smith, S. J., and White, H. D. (1985) *J. Biol. Chem. 260*, 15146−15155.
10. Weeds, A. G., and Taylor, R. S. (1975) *Nature 257*, 54−56.
11. White, H. D. (1982) *Methods Enzymol. 85* (Pt. B), 698−708.
12. Zhang, X.-Z., Strand, A., and White, H. D. (1989) *Anal. Biochem. 176*, 427−431.
13. Dyson, R. D., and Isenberg, I. (1971) *Biochemistry 10*, 3233−3241.
14. Leatherbarrow, R. J. (1992) *Grafit*, Version 3.0, Erithacus Software Ltd., Staines, U.K.
15. White, H. D., Belknap, B., and Jiang, W. (1993) *J. Biol. Chem. 268*, 10039−10045.
16. Pate, E., Franks Skiba, K., White, H., and Cooke, R. (1993) *J. Biol. Chem. 268*, 10046−10053.
17. Taylor, E. W. (1977) *Biochemistry 16*, 732−739.
18. Eccleston, J. F., and Trentham, D. R. (1979) *Biochemistry 13*, 2896−2904.
19. Belknap, B., Wang, X.-Q., and White, H. (1994) *Biophys. J. 66*, 79a.
20. Sleep, J. A., and Hutton, R. L. (1978) *Biochemistry 17*, 5423−5430.
21. Rosenfeld, S. S., and Taylor, E. W. (1984) *J. Biol. Chem. 259*, 11908−11919.
22. Tesi, C., Kitagishi, K., Travers, F., and Barman, T. (1991) *Biochemistry 30*, 4061−4067.
23. Fischer, A. J., Smith, C. A., Thoden, J. B., Smith, R., Sutoh, K., Holden, H., and Rayment, I. (1995) *Biochemistry 34*, 8960−8972.
24. Sellers, J. R., and Goodson, H. V. (1995) *Protein Profile 2*, 1323−1423.
25. He, Z., Chillingworth, R. K., Brune, M., Corrie, J. E. T., Trentham, D. R., Webb, M. R., and Ferenczi, M. A. (1997) *J. Physiol. 501*, 125−148..
26. Millar, N. C., and Homsher, E. (1990) *J. Biol. Chem. 265*, 20234−20240.
27. Walker, J. W., Lu, Z., and Moss, R. L. (1992) *J. Biol. Chem. 267*, 2459−2466.
28. Pate, E., White, H., and Cooke, R. (1993) *Proc. Natl. Acad. Sci. U.S.A. 90*, 2451−2455.
29. Glyn, H., and Sleep, J. A. (1985) *J. Physiol. (London) 365*, 259−276.
30. Potma, E. J., Steinem, G. J., Barends, J. P., and Elzinga, G. (1994) *J. Physiol. (London) 474*, 303−317.
31. Stephenson, D. G., Stewart, A. W., and Wilson, G. J. (1989) *J. Physiol. 410*, 351−366.
32. Ferenczi, M. A., Homsher, E., and Trentham, D. R. (1984) *J. Physiol (London) 352*, 575−599.
33. Ferenczi, M. A. (1986) *Biophys. J. 50*, 471−477.
34. Herrmann, C., Lionne, C., Travers, F., and Barman, T. (1994) *Biochemistry 33*, 4148−4154.
35. Lionne, C., Brune, M., Webb, M. R., Travers, F., and Barman, T. (1995) *FEBS Lett. 364*, 59−62.
36. Ma, Y. Z., and Taylor, E. W. (1994) *Biophys. J. 66*, 1542−1553.
37. Belknap, B., Wang, X.-Q., and White, H. D. (1992) *Biophys. J. 61*, 440a.
38. Regnier, M., and Homsher, E. (1996) *Biophys. J. 70*, 290a.
39. Jiang, W. (1995) Ph.D. Thesis, Eastern Virginia Medical School, Norfolk, VA.
40. Zhang, X.-Z, Jiang, W., and White, H. D. (1992) *Biophys. J. 61*, 440a.
41. Burton, K., and Sleep, J. (1988) *Biophys. J. 51*, 6a.
42. Cooke, R., White, H., and Pate, E. (1994) *Biophys. J. 66*, 778−788.

BI970540H